AEM
Journals.ASM.org

Microbiological Oxidation of Antimony(III) with Oxygen or Nitrate by Bacteria Isolated from Contaminated Mine Sediments

Lee R. Terry,[a] Thomas R. Kulp,[a] Heather Wiatrowski,[b]* Laurence G. Miller,[c] Ronald S. Oremland[c]

Department of Geological Sciences and Environmental Studies, Binghamton University, SUNY, Binghamton, New York, USA[a]; Department of Biology, Clark University, Worcester, Massachusetts, USA[b]; U.S. Geological Survey, Menlo Park, California, USA[c]

Bacterial oxidation of arsenite [As(III)] is a well-studied and important biogeochemical pathway that directly influences the mobility and toxicity of arsenic in the environment. In contrast, little is known about microbiological oxidation of the chemically similar anion antimonite [Sb(III)]. In this study, two bacterial strains, designated IDSBO-1 and IDSBO-4, which grow on tartrate compounds and oxidize Sb(III) using either oxygen or nitrate, respectively, as a terminal electron acceptor, were isolated from contaminated mine sediments. Both isolates belonged to the *Comamonadaceae* family and were 99% similar to previously described species. We identify these novel strains as *Hydrogenophaga taeniospiralis* strain IDSBO-1 and *Variovorax paradoxus* strain IDSBO-4. Both strains possess a gene with homology to the *aioA* gene, which encodes an As(III)-oxidase, and both oxidize As(III) aerobically, but only IDSBO-4 oxidized Sb(III) in the presence of air, while strain IDSBO-1 could achieve this via nitrate respiration. Our results suggest that expression of *aioA* is not induced by Sb(III) but may be involved in Sb(III) oxidation along with an Sb(III)-specific pathway. Phylogenetic analysis of proteins encoded by the *aioA* genes revealed a close sequence similarity (90%) among the two isolates and other known As(III)-oxidizing bacteria, particularly *Acidovorax* sp. strain NO1. Both isolates were capable of chemolithoautotrophic growth using As(III) as a primary electron donor, and strain IDSBO-4 exhibited incorporation of radiolabeled [^{14}C]bicarbonate while oxidizing Sb(III) from Sb(III)-tartrate, suggesting possible Sb(III)-dependent autotrophy. Enrichment cultures produced the Sb(V) oxide mineral mopungite and lesser amounts of Sb(III)-bearing senarmontite as precipitates.

Antimony (Sb) is a redox-sensitive toxic trace metalloid that is of increasing environmental concern around the world, particularly in areas where it is mined for use in an array of products, including semiconductors, fire retardants, batteries, munitions, automobile brake linings, cable sheathing, and solders (1–3). The element is classified as a priority pollutant by the U.S. Environmental Protection Agency (EPA), which sets the current maximum contaminant level for drinking water at 6 μg/liter. Chronic Sb exposure can result in health impacts similar to those of arsenic (As) poisoning, such as damage to the heart, liver, lungs, and kidneys (4). Antimony and As are both group 15 metalloids, thereby sharing a number of chemical properties in addition to their toxicity. They both typically exist in the +5 valence state in oxygenated environments and in the +3 state under anoxic conditions. These variations in oxidation state influence the toxicity, bioavailability, and environmental mobility of the two metalloids. Antimony and As are both chalcophilic elements that often cooccur in association with sulfide minerals around hydrothermal ore deposits. Ecosystems surrounding mining and smelting operations can therefore become contaminated due to oxidative dissolution of Sb- and As-sulfides in sulfidic mine tailings (5–8).

Biologically mediated oxidative and reductive transformations of As between the pentavalent As(V) and trivalent As(III) oxidation states are well studied in a wide range of phylogenetically diverse prokaryotes (9, 10). Four operons from bacteria are implicated in transformations of As. The *ars* and *arr* operons are involved in the reduction of As(V) to As(III), while the *aio* (formerly called *aox*) and *arx* operons are associated with the oxidation of As(III) to As(V). The *ars* operon confers cellular resistance to As by way of a periplasmic As(V) reductase (*arsC*) and an As(III) efflux pump (*arsB*) that also removes Sb(III) from the cell (11, 12). The *arr* system encodes a reductase that permits anaerobic respiration, which couples dissimilatory As(V) reduction to the oxidation of various organic and inorganic electron donors (9, 10). The converse reaction, As(III) oxidation, can serve as a detoxification mechanism in heterotrophs or as a source of electrons to drive chemoautotrophy with oxygen as a terminal electron acceptor (9). Aerobic As(III) oxidation is catalyzed by an inner-membrane-bound oxidase (Aio) that is encoded by the *aio* operon (13). Oxidation of As(III) can also donate electrons to drive chemoautotrophy in anoxic settings via the reduction of nitrate (14, 15) and also to fuel anoxygenic photosynthesis in purple sulfur bacteria (16, 17). Both of these processes proceed via enzymes encoded by the *arx* operon (18–20). Proteins encoded on the *arr*, *aio*, and *arx* operons are complex iron sulfur molybdoproteins (CISMs). CISMs form a family of approximately 14 types of proteins, including enzymes used for the respiration of dimethyl sulfoxide (DMSO), As(V), As(III), nitrate, and selenate, as well as the enzymes biotin sulfoxide reductase, pyrogallol transhydroxylase, and ethylbenzene dehydrogenase (21, 22).

Received 11 June 2015 **Accepted** 29 September 2015

Accepted manuscript posted online 2 October 2015

Citation Terry LR, Kulp TR, Wiatrowski H, Miller LG, Oremland RS. 2015. Microbiological oxidation of antimony(III) with oxygen or nitrate by bacteria isolated from contaminated mine sediments. Appl Environ Microbiol 81:8478–8488. doi:10.1128/AEM.01970-15.

Editor: H. L. Drake

Address correspondence to Thomas R. Kulp, tkulp@binghamton.edu.

* Present address: Heather Wiatrowski, 34 Oakwood Ave., Auburn, Massachusetts, USA.

Copyright © 2015, American Society for Microbiology. All Rights Reserved.

Compared to As geomicrobiology, our understanding of the role that microbes play in the environmental cycling of Sb remains incomplete. However, results from an increasing number of recent studies suggest that microbiological processes similar to those described for As also drive a biogeochemical Sb cycle in nature. For example, one recent study has reported growth coupled to the dissimilatory reduction of Sb(V) to Sb(III) as a respiratory electron acceptor in a *Firmicutes* isolate from Mono Lake, CA (23). Likewise, our group recently demonstrated respiratory anoxic Sb(V) reduction by a microbial community within Sb-contaminated sediments from Stibnite Mine, ID (24). Studies on the microbiological oxidation of Sb(III) have largely focused on Sb-resistant bacteria that employ this biotransformation as an apparent cellular detoxification mechanism while growing as heterotrophs (25–28). Reports of Sb(III) oxidation that is coupled to the conservation of energy for chemoautotrophic growth are restricted to some earlier studies (29–31) regarding the bacterial isolate *Stibiobacter senarmontii*, which was isolated from a stibnite ore body and grew by fixing CO_2 while using Sb(III) as an electron donor. The studies with *S. senarmontii* were conducted prior to the widespread application of modern genomic methods, and no further characterization of that organism or any other Sb(III)-oxidizing autotroph has since been reported. Recent work by Wang et al. (32) demonstrated that a mutation in the *aioA* structural gene reduces the ability to oxidize Sb(III) by approximately one-third in *Agrobacterium tumefaciens* strain 5A. This suggests that *aioA* may be partially involved with Sb(III) oxidation but also implicates other unknown pathways. One such novel Sb(III) oxidase belonging to the short-chain dehydrogenase/reductase family of enzymes, and designated *anoA*, was recently identified by Li et al. (33) and was found to be widely distributed among bacteria, including some that are able to oxidize Sb(III).

In this contribution, we report the isolation and characterization of two bacterial strains from Stibnite Mine, *Hydrogenophaga taeniospiralis* strain IDSBO-1 and *Variovorax paradoxus* strain IDSBO-4. Strain IDSBO-4 grows as an aerobe and oxidizes Sb(III) to Sb(V) during growth on potassium antimony(III) tartrate. We report the fixation of radiolabeled [^{14}C]bicarbonate during growth and oxidation of Sb(III) by strain IDSBO-4, suggesting an autotrophic process. Strain IDSBO-1 grows as an anaerobe on potassium antimony(III) tartrate with nitrate as an electron acceptor and oxidizes Sb(III) to Sb(V) coupled to the reduction of nitrate. This study thereby expands our understanding of bacterial pathways for Sb(III) oxidation and contributes to our emerging picture of the biogeochemical redox cycle that controls the environmental behavior of Sb.

MATERIALS AND METHODS

Study area and sample collection. We isolated bacteria from sediment that was collected in the highly As- and Sb-contaminated Stibnite/Yellow Pine mining area of Idaho during July 2012. Antimony, gold, and tungsten mining from the early 1900s until the late 1990s has resulted in waste ore and mine tailings being deposited over approximately 50% of the 3,000-acre Stibnite Mine site (34). Sediment was collected from a seasonally flooded shallow seep near the edge of a large tailings pile (designated "Heap Seep" [HS]) and from a permanently flooded small pond that occurs in an abandoned stream channel near the tailings piles (designated "Channel Pond" [CP]). A detailed description of the study area and the locations of the HS and CP is provided by Dovick et al. (6). Extremely elevated dissolved and sedimentary concentrations of As and Sb in these locations, measured in samples collected during the same sampling trip, were previously reported by Dovick et al. (6) and are summarized in Table 1. Sediment samples were collected in sealed glass jars (1 pint) and transported to the laboratory under chilled conditions. Samples were stored in the dark at 5°C for up to 11 months prior to use in sediment microcosm experiments.

TABLE 1 Concentrations of dissolved and sedimentary As and Sb, along with pH values, for the two Stibnite Mine sites sampled in this study[a]

Site designation	pH	Concn of metalloid in:			
		Surface water (μM)		Sediment (mg/kg)	
		As	Sb	As	Sb
Heap Seep	9.4	144.6	8.6	1,388.8	43.1
Channel Pond	8.2	2.3	2.6	292.6	203.5

[a] As reported by Dovick et al. (6).

Sediment microcosms. Microcosms were prepared to assess the capacity for the sedimentary microbial community to oxidize As(III) or Sb(III). Microcosms (30-ml total volume) were prepared with artificial freshwater medium SeFr1 (35) amended to 2 mM As(III) (added as $NaAsO_2$) or Sb(III) [added as potassium antimony(III) tartrate, $C_8H_4K_2O_{12}Sb_2{\cdot}3H_2O$], and inoculated with sediment from either the HS or CP locations (sediment-to-medium ratio, 1:19). Potassium antimony(III) tartrate ($C_8H_4K_2O_{12}Sb_2{\cdot}3H_2O$) has been used as an Sb(III) source in several previous microbiological studies (e.g., see references 25–27 and 32) owing to the poor aqueous solubility of other Sb(III) compounds. The tartrate form also allows Sb(III) to be solubilized without interfering with its cellular uptake, extrusion, or interaction with regulatory proteins (26). Abiotic control microcosms were prepared identically to live trials but without sediment inoculum or by twice autoclaving (121°C, 250 kPa, 50 min) subsequent to the addition of sediment inocula. Microcosms were capped with a permeable foam stopper to allow exchange with the atmosphere and incubated in the dark at 27°C with gentle rotary shaking for ~8 days. The microcosms were periodically subsampled (0.5 ml) with sterile Pasteur pipettes and filtered by centrifugation (14,000 rpm, 2 min) in 0.45-μm-pore nylon filter microcentrifuge tubes (Costar, Inc.) prior to analysis to monitor changes in dissolved $C_8H_4K_2O_{12}Sb_2{\cdot}3H_2O$, Sb(V), As(III), and As(V).

Enrichment cultures. Aliquots (0.1 ml) from live As(III)- and Sb(III)-oxidizing microcosms were inoculated into culture tubes prepared with 13 ml of SeFr1 medium amended to 2 mM As(III) (added as $NaAsO_2$) or Sb(III) (added as 1 mM $C_8H_4K_2O_{12}Sb_2{\cdot}3H_2O$) and capped with permeable foam stoppers. Enrichments were incubated statically, subsampled, and analyzed as previously described for sediment microcosms. After 12 days, a loss of As(III) or $C_8H_4K_2O_{12}Sb_2{\cdot}3H_2O$ and increasing turbidity were observed in all live enrichment cultures.

Secondary enrichments were prepared with the SeFr1 medium composition modified by omitting yeast extract to eliminate this potential organic substrate. Secondary enrichments were constructed with 0.1 ml of primary enrichment culture and 13 ml medium. As with the primary enrichments, the yeast-free enrichments showed progressive loss of 2 mM As(III) or Sb(III) over 10 days. Following the enrichment experiments, solid precipitated mineral residues were collected from the cultures by filtration and dried at 60°C for 48 h prior to X-ray diffraction (XRD) analysis.

Isolation of ISDBO-1 and IDSBO-4. We obtained pure cultures of As(III)- and Sb(III)-oxidizing organisms by streaking the secondary enrichments onto agar plates prepared with yeast extract-free medium amended with 1.4 mM sodium bicarbonate, vitamins (36), 2% agar, and 2 mM As(III) or 1 mM $C_8H_4K_2O_{12}Sb_2{\cdot}3H_2O$. The plates were incubated at 27°C in the air. Colonies were observed on the plates within 15 days, and these colonies were restreaked several times on fresh agar to obtain purity.

Growth conditions. Isolates that grew on As(III)-amended agar appeared as irregular, colorless, sheet-like colonies, while the Sb(III)-

amended plates yielded whitish-yellow, raised, circular colonies. Each of these colony types was picked and resuspended into both oxic and anoxic culture tubes (prepared in triplicate) that contained the sulfate-free freshwater medium SeFr2 (37), which was prepared with yeast extract omitted and amended with vitamins (36) and 2 mM sodium bicarbonate. The SeFr2 medium was chosen for the growth experiments in order to eliminate sulfate as a potential electron acceptor under anoxic conditions. Anoxic culture tubes were prepared by bubbling the liquid medium (200 ml for 20 min) with O_2-free N_2 and transferring 13 ml into each tube under a flow of N_2 (38). Tubes were amended with 2 mM As(III) and/or 2 mM Sb(III) (added as 1 mM $C_8H_4K_2O_{12}Sb_2{\cdot}3H_2O$), and anoxic tubes also received 2 mM nitrate (as $NaNO_3$). To determine if tartrate present in the Sb(III) stock could support growth, we also prepared a set of oxic and anoxic tubes that were amended with 1 mM potassium sodium tartrate ($KNaC_4H_4O_6{\cdot}4H_2O$) in lieu of As(III) or $C_8H_4K_2O_{12}Sb_2{\cdot}3H_2O$. Cultures were incubated and subsampled as described above to measure As(III) and Sb(III) oxidation activity, loss of tartrate, and the reduction of nitrate to nitrite. Quantification of cell populations and growth was achieved by direct counting using fluorescence microscopy (39).

Radioisotope experiments. Radioisotope experiments with [^{14}C]bicarbonate ($H^{14}CO_3^-$) were conducted using methods similar to those detailed by Oremland et al. (14). Culture tubes were prepared containing 10 ml sterile SeFr2 medium, without yeast extract. Strain IDSBO-4 was grown aerobically on Sb(III) as described above, and 0.5 ml of actively growing culture was used as the inoculum for the radioisotope experiment. Antimony-amended tubes received 2 mM Sb(III) addition. Triplicate sets of Sb(III)-amended and nonamended tubes were inoculated, while an additional set of control tubes received 2 mM Sb(III) but no inoculum. All tubes were injected with $H^{14}CO_3^-$ (total activity, 5 μCi/tube [185,000 Bq]). Duplicate tubes were constructed without the tracer to monitor Sb(III) oxidation during the experiment in nonradioactive samples. After 6 days of incubation in the dark (25°C), complete oxidation of Sb(III) to Sb(V) was observed in the monitoring tubes and the experiment was terminated. The contents of each tube were pressure filtered (pore size, 0.45 μm) to collect the cells from suspension, the filters were acid fumed overnight in a desiccator, and the radioactivity associated with acid-insoluble carbon was counted by liquid scintillation spectrometry.

Analytical. Arsenic(III) and As(V) were measured by high-performance liquid chromatography (HPLC) using a Dionex Ultimate3000 high-performance liquid chromatograph with UV detection (210 nm) and two inline ion-exchange columns (Bio-Rad Aminex HPX-87H followed by Hamilton PRP X300) with 0.016 N H_2SO_4 eluent flowing at 0.6 ml/min (51). Potassium antimony(III) tartrate and potassium sodium tartrate were also quantified by HPLC. Under the specified conditions, both tartrate compounds eluted at 13.1 min, and we obtained a linear calibration ($R^2 > 0.94$) in the range of 10 to 500 μM using standards made from each compound (data not shown). Antimony(V), nitrate, and nitrite were measured by ion chromatography (IC) with conductivity detection as noted by Hoeft et al. (40) using a Dionex ICS-2000 ion chromatograph configured with a Dionex AS-18 column and 32 mM KOH mobile phase flowing at 1.0 ml/min. Under these conditions, Sb(V) eluted at 2.8 min, immediately after the injection peak. We obtained a linear calibration ($R^2 = 0.968$) for Sb(V) in the range from 10 to 500 μM using standards made from $KSbO_3{\cdot}3H_2O$ (data not shown). Powder X-ray diffraction analysis of precipitates from Sb(III)-oxidizing cultures were conducted using a Phillips Xpert PW3040-MPD diffractometer.

Genomic analyses. Bacterial DNA was extracted using the Mo Bio Ultraclean microbial DNA isolation kit (Mo Bio Laboratories, Inc., Carlsbad, CA). 16S rRNA genes were amplified using the 27F and 1492R primers described by Polz and Cavanaugh (41). *aioA* sequences were amplified with primer set 2 as described by Inskeep et al. (42). Sequencing was performed by Macrogen (Cambridge, MA). Contigs were assembled and proteins were translated using MacVector 12.7.5 (Oxford Molecular, Cary, NC). The lengths of the partial 16S rRNA sequences from strains IDSBO-1 and IDSBO-4 were 1,400 and 1,454 nucleotides, respectively.

Evolutionary analyses were performed using Mega 6.0 (43) with 250 bootstrap replicates performed (44). Alignments were constructed using MUSCLE (45). Initial trees for the heuristic search were obtained by applying the neighbor-joining method to a matrix of pairwise distances estimated using a JTT model. Phylogenetic analysis of partial 16S rRNA was inferred using the maximum likelihood method based on the general time reversible model. The tree with the highest log likelihood (−5,159.3994) was selected. Initial trees for the heuristic search were obtained automatically by applying Neighbor-Join and BioNJ algorithms to a matrix of pairwise distances estimated using the maximum composite likelihood (MCL) approach and then selecting the topology with superior log likelihood value. A discrete gamma distribution was used to model evolutionary rate difference among sites (5 categories [+G; parameter = 0.1264]). The rate variation model allowed for some sites to be evolutionarily invariable ([+I]; 64.5443% of sites). The analysis involved 17 nucleotide sequences. The codon positions included were 1st + 2nd + 3rd + noncoding. All positions containing gaps and missing data were eliminated. There were a total of 1,339 positions in the final data set. Evolutionary histories for AioA protein sequences were inferred using the maximum likelihood method described by Whelan and Goldman (46). A discrete gamma distribution was used to model evolutionary rate differences among sites.

Nucleotide sequence accession numbers. The NCBI accession numbers for the partial 16S rRNA genes for *H. taeniospiralis* strain IDSBO-1 and *V. paradoxus* strain IDSBO-4 are KM199760 and KM199761, respectively. The lengths of the partial 16S rRNA sequences from strains IDSBO-1 and IDSBO-4 were 1,400 and 1,454 nucleotides, respectively. The accession numbers for the partial *aioA* genes and translated proteins from strains IDSBO-1 and IDSBO-4 are KM199762 and KM199763, respectively.

RESULTS

Sediment microcosms. Live sediment microcosms from both the CP (Fig. 1A) and HS (data not shown) localities demonstrated complete oxidation of 2.5 mM concentrations of As(III) to As(V) within 4 days under As(III)-amended conditions. The recovery rates of lost As(III) as dissolved As(V) were 77% in CP microcosms and 81% in HS microcosms. In microcosms amended with 1.5 mM $C_8H_4K_2O_{12}Sb_2{\cdot}3H_2O$, rapid and complete loss of that compound from solution was observed within 4 days but without significant aqueous recovery of Sb(V) (Fig. 1B). Subsequent amendments of As(III) or $C_8H_4K_2O_{12}Sb_2{\cdot}3H_2O$ were also rapidly depleted within 3 to 4 days. Control microcosms that were prepared identically to live microcosms but sterilized after sediment inoculation (Fig. 1), or which were prepared without sediment inoculum (data not shown), showed no activity. The loss of $C_8H_4K_2O_{12}Sb_2{\cdot}3H_2O$ from solution in the microcosms, in the absence of a corresponding recovery of aqueous Sb(V), indicated removal of Sb species via precipitation. We identify the mineral form and oxidation state of Sb precipitated by these microorganisms, in enrichment culture, in the following section.

Enrichment cultures and isolation of Sb(III)-oxidizing bacteria. An initial set of enrichment cultures was established by inoculating microcosms that utilized $C_8H_4K_2O_{12}Sb_2{\cdot}3H_2O$ into SeFr1 medium that contained yeast extract (0.5 g/liter) and 2 mM As(III) or Sb(III) (as $C_8H_4K_2O_{12}Sb_2{\cdot}3H_2O$). Enrichment cultures inoculated from both CP (Fig. 2) and HS (data not shown) microcosms rapidly oxidized two subsequent amendments of Sb(III) or As(III) and exhibited increasing turbidity over 12 days. A yellowish precipitate formed by 5 days in all live Sb(III)-amended cultures and progressively darkened to a light orange by 14 days (Fig. 3A). X-ray diffraction analysis determined that the precipitate was primarily composed of the Sb(V)-bearing mineral

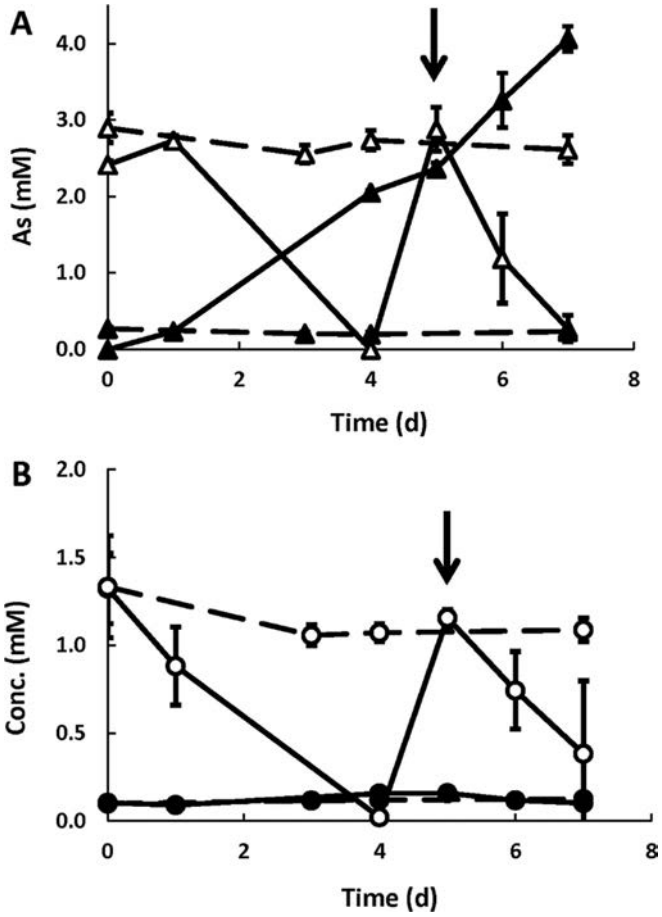

FIG 1 (A) Arsenic-amended sediment microcosms oxidized 2.5 mM As(III) (open triangles) to As(V) (closed triangles) in live microcosms (solid lines). (B) Antimony(III)-amended microcosms removed $C_8H_4K_2O_{12}Sb_2{\cdot}3H_2O$ (open circles) from solution in live slurries (solid lines) with poor recovery as dissolved Sb(V) (closed circles). No activity occurred in autoclaved control slurries under any condition (dashed lines). Arrows denote the timing of supplemental As(III) or Sb(III) amendment. Symbols represent the means from three replicate samples, and error bars represent ±1 standard deviation. The absence of bars indicates that the error was smaller than the sample.

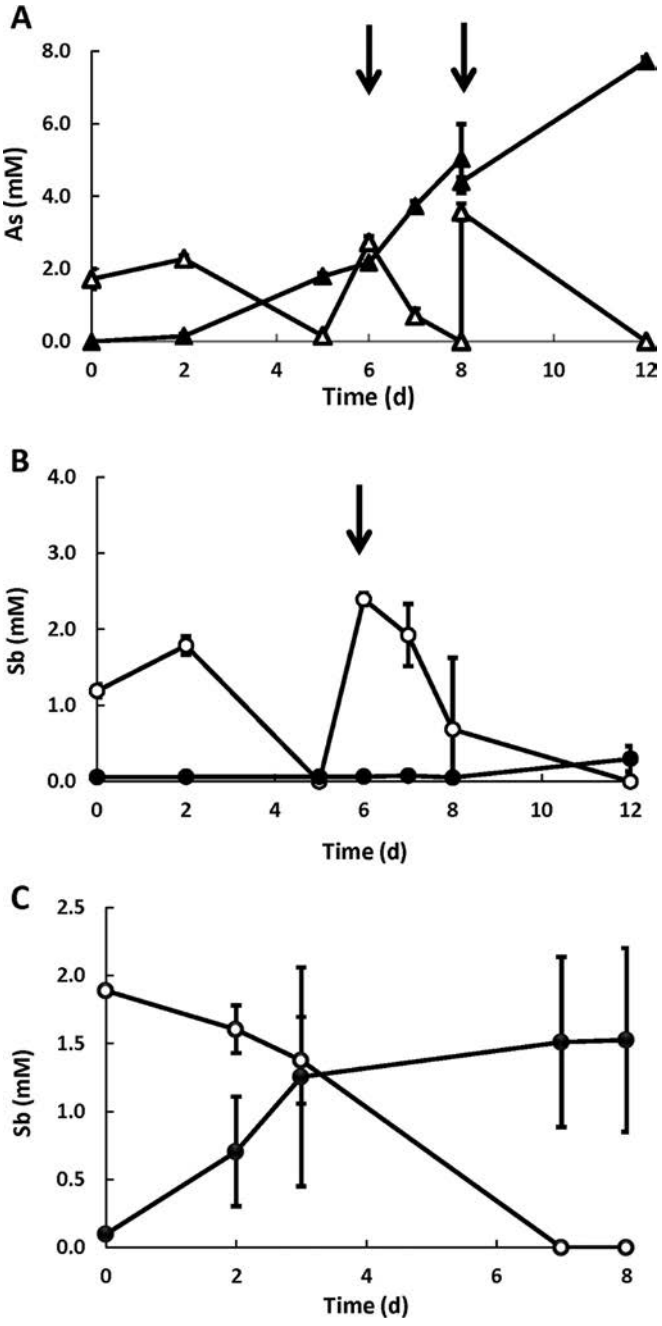

FIG 2 (A) Oxidation of As(III) (open triangles) to As(V) (closed triangles) in enrichment cultures inoculated from Stibnite Mine sediment microcosms. (B) Removal of Sb(III) as $C_8H_4K_2O_{12}Sb_2{\cdot}3H_2O$ (open circles) from solution in enrichment cultures amended with yeast extract (0.5 g liter^{-1}) was accompanied by poor recovery as aqueous Sb(V) (closed circles) and by the precipitation of Sb oxide mineral phases (Fig. 3). (C) The elimination of yeast extract in subsequent transfers of the enrichments resulted in greatly increased recovery of dissolved Sb(V) during Sb(III) oxidation. Arrows denote the timing of supplemental As(III) or Sb(III) amendment. Symbols represent the means from three replicate samples, and error bars represent ±1 standard deviation. The absence of bars indicates that the error was smaller than the sample.

mopungite [$NaSb(OH)_6$], which accounted for 87% and 94% of precipitated Sb species in CP (Fig. 3B) and HS (data not shown) enrichments, respectively. The remainder of precipitated Sb was comprised of Sb(III)-bearing senarmontite (Sb_2O_3). No activity was observed in control tubes that lacked Sb(III) or As(III) amendment or in heat-sterilized controls (data not shown). Recovery of oxidized As(III) as aqueous As(V) was >90% in these enrichments (Fig. 2A), whereas aqueous recovery of Sb(V) in Sb(III)-amended enrichments was <12% (Fig. 2B). Enrichment cultures that were serially diluted into yeast extract-free medium continued to oxidize millimolar concentrations of Sb(III) and As(III) under aerobic conditions, with observable increase in turbidity (data not shown). The elimination of yeast extract from the media resulted in significantly enhanced aqueous Sb(V) recovery in these secondary enrichments. In yeast extract-free media, the aqueous Sb(V) recovery rates were 75% for CP cultures (Fig. 2C) and 59% for HS (data not shown). Antimony(III)-amended cultures developed noticeably less yellowish-orange precipitates than were observed in the initial enrichments. X-ray diffraction analysis of these precipitates in the secondary CP enrichments identified the mineral forms as 72% mopungite and 28% senarmontite (data not shown).

The secondary enrichment cultures were streaked onto agar

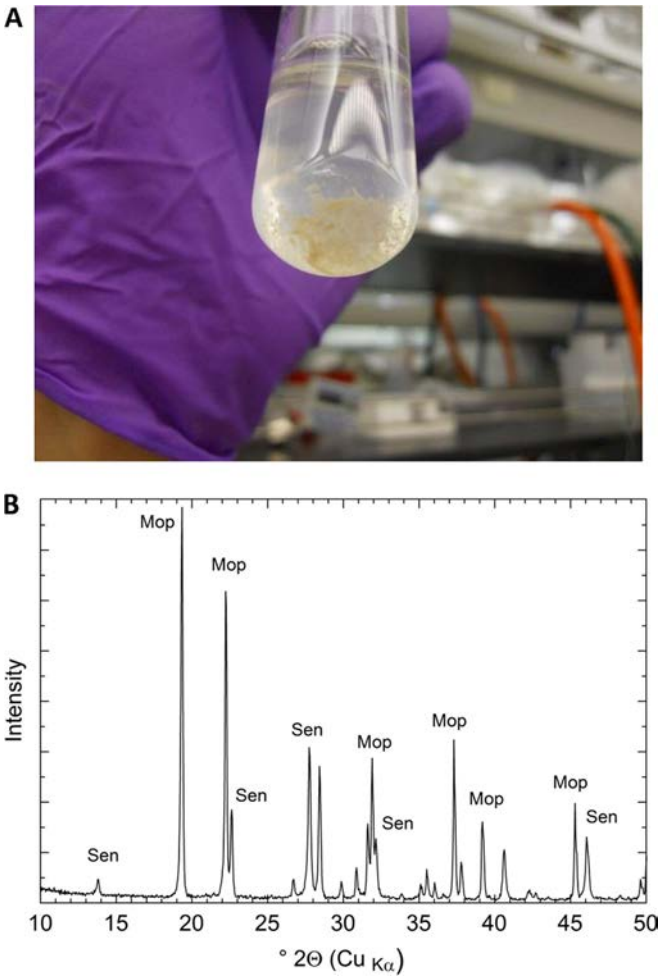

FIG 3 (A) Yellow precipitates formed in Sb(III)-amended live cultures after ~10 days of incubation. (B) X-ray diffraction pattern of the precipitate from Sb(III)-amended CP enrichments. Major peaks corresponding to mopungite [$NaSb(OH)_6$] and senarmontite (Sb_2O_3) are labeled. Mop, mopungite; Sen, senarmontite. The smaller unlabeled peaks correspond to sylvite (KCl) and arcanite (K_2SO_4), which precipitated from the growth medium.

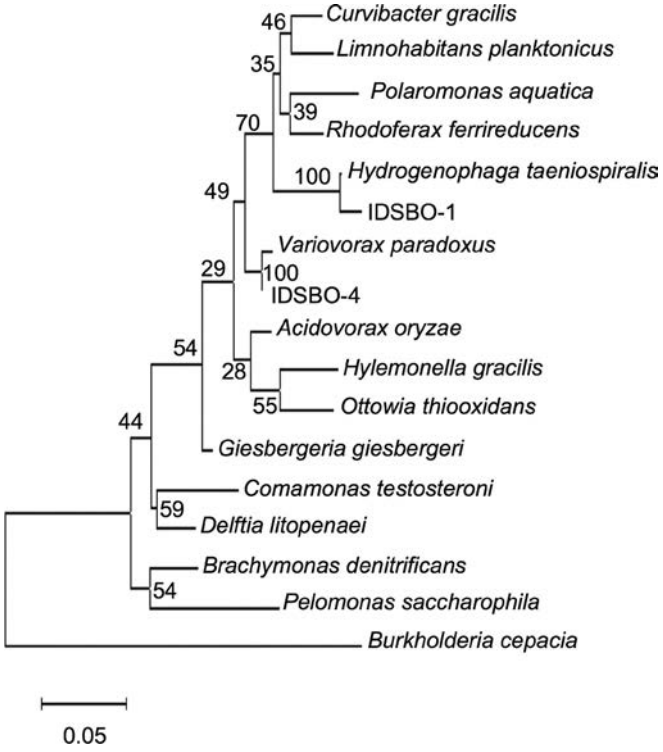

FIG 4 Evolutionary analyses based on 16S rRNA sequences. Strain names and NCBI accession numbers are as follows: IDSBO-1, KM199760.1; IDSBO-4, KM199761.1; *Acidovorax oryzae* strain FC-143, NR_043752.1; *Brachymonas denitrificans* strain AS-P1, NR_025834.1; *Comamonas testosteroni* strain H18, EU887829.1; *Curvibacter gracilis* strain 7-1, NR_028655.1; *Delftia litopenaei* strain wsw-7, NR_108843.1; *Giesbergeria giesbergeri* strain NBRC 13959, NR_113642.1; *Hydrogenophaga taeniospiralis* strain NBRC, NR_114131.1; *Hylemonella gracilis* strain NBRC 14920, NR_113697.1; *Limnohabitans planktonicus* strain II-D5, NR_125541.1; *Ottowia thiooxydans* strain K11, NR_029001.1; *Pelomonas saccharophila* strain DSM 654, NR_115052.1; *Polaromonas aquatica* strain CCUG 39402, NR_042404.1; *Rhodoferax ferrireducens* T118, NR_114646.1; *Variovorax paradoxus* S110, NR_074654.1; and *Burkholderia cepacia* strain ATCC 53130, AY741362.1. The percentage of trees in which the associated taxa clustered together is shown next to the branches. The tree is drawn to scale, with branch lengths measured in the number of substitutions per site.

plates to obtain bacterial isolates. Growth of bacterial colonies was observed on the plates within 15 days. Two bacterial strains capable of Sb(III) oxidation were successfully isolated by repeated plating and resuspension in liquid medium. The first, designated strain IDSBO-1, is a rod-shaped bacterium that was derived from CP sediment and isolated on As(III)-amended plates. The second, strain IDSBO-4, possesses a coccus-shaped cell morphology and was isolated from HS sediments on Sb(III)-amended plates.

Genomic analysis. The 16S rRNA sequence analysis conducted by the Ribosomal Database Classifier program (47) set to 95% confidence resulted in both strain IDBO-1 and strain IDSBO-4 being placed in the family *Comamonadaceae*. The 16S rRNA sequence of strain IDSBO-1 was 99% identical to *Hydrogenophaga taeniospiralis* strain NBRC 102512 (NCBI accession no. NR_114131.1), while strain IDSBO-4 was 99% identical to *Variovorax paradoxus* S110 (NCBI accession no. NR_074654.1) (Fig. 4). We therefore assign our isolated strains to these two species, respectively. High-quality DNA sequences were also obtained and amplified from a region of the genomes of the two strains that aligned with amino acids 89 to 186 of the AioA protein from *Rhizobium* sp. strain NT26. Phylogenetic analysis of the amplified sequences solidly places them within a clade of AioA sequences on a node with 90% bootstrap support and further clusters these sequences with that of *Acidovorax* sp. strain NO1, which is also in the family *Comamonadaceae*. Closer analysis of these sequences reveals their homology to AioA from other members of the family *Comamonadaceae*, including genera of *Polaromonas*, *Acidovorax*, and *Hydrogenophaga*, on a node with strong bootstrap support (Fig. 5).

Growth experiments. *H. taeniospiralis* strain IDSBO-1 demonstrated growth on potassium antimony(III) tartrate, along with Sb(III) oxidation, coupled to the reduction of nitrate under anoxic conditions. Removal of 0.5 mM $C_8H_4K_2O_{12}Sb_2{\cdot}3H_2O$ from solution was concurrent with a loss of 2 mM nitrate after 18 days (Fig. 6A). The Sb(III) was partially recovered (48%) as aqueous Sb(V). The remaining Sb(III) was lost from solution due to precipitation as Sb(III)-bearing senarmontite (data not shown), which formed a white residue in the live cultures. Nitrite formed

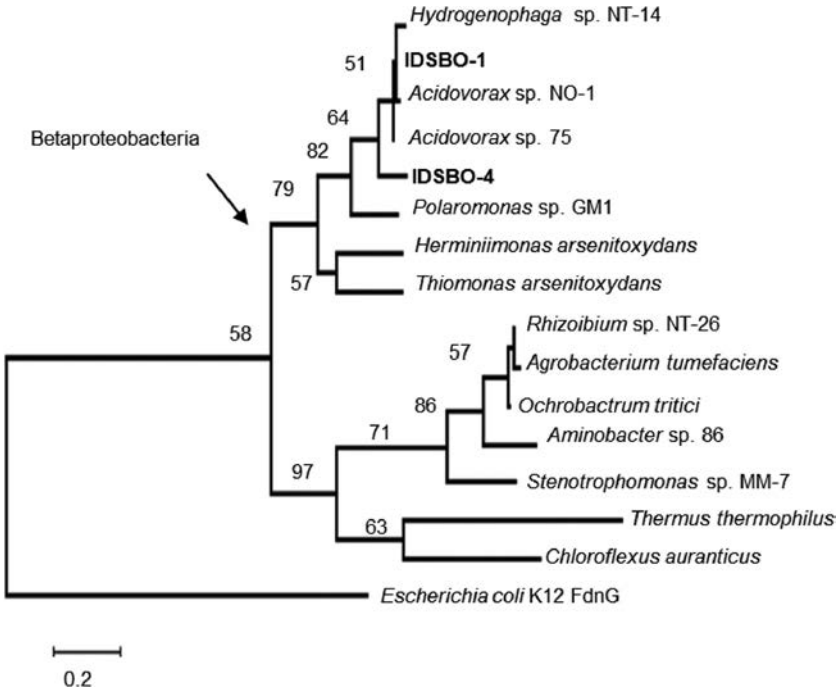

FIG 5 Phylogenetic comparison of AioA proteins from *H. taeniospiralis* strain IDSBO-1 and *V. paradoxus* strain IDSBO-4 to those possessed by other As(III)-oxidizing bacteria. Prior to analyses, proteins were aligned and trimmed to the region homologous to amino acids 89 to 186 of the AioA protein from *Rhizobium* sp. strain NT26. Numbers at nodes indicate the percentage of trees in which the associated taxa were clustered. The tree is drawn to scale, with branch lengths measured in the number of substitutions per site. The formate dehydrogenase N alpha subunit (FdnG) protein from *Escherichia coli* K-12 was used as an outgroup.

as a transient reduction product of nitrate and reached a maximum concentration of 0.75 mM at 13 days before presumably being further reduced. These activities corresponded to a roughly 150-fold increase in cell density (as quantified by direct counting). Strain IDSBO-1 grew at a similar rate when $KNaC_4H_4O_6{\cdot}4H_2O$ was provided as a substrate in lieu of $C_8H_4K_2O_{12}Sb_2{\cdot}3H_2O$ in nitrate-reducing cultures (Fig. 6B). No loss of $C_8H_4K_2O_{12}Sb_2{\cdot}3H_2O$, oxidation of Sb(III), reduction of nitrate, or precipitation of senarmontite occurred in autoclaved controls, and no cell growth was observed in controls that did not receive either $C_8H_4K_2O_{12}Sb_2{\cdot}3H_2O$ or $KNaC_4H_4O_6{\cdot}4H_2O$ (data not shown). Strain IDSBO-1 also exhibited a capacity for anaerobic, chemoautotrophic growth via As(III) oxidation with nitrate, as well as aerobic autotrophy using As(III) and oxygen. Figure 6C shows a 24-fold increase in cell density after 15 days coupled to the anaerobic oxidation of 2 mM As(III) to As(V) (84% recovery) and the reduction of 2 mM nitrate to nitrite (78% recovery). Figure 6D shows an 11-fold growth of cells associated with the oxidation of a total of 5 mM As(III) to As(V) (86% recovery) over 10 days in the air. Strain IDSBO-1 did not oxidize Sb(III) aerobically (data not shown). However, strain IDSBO-1 preferentially oxidized As(III) in anoxic cultures amended with nitrate and equimolar concentrations of As(III) and Sb(III), with no detectable Sb(III) oxidation occurring until after 51% of the As(III) amendment had been oxidized to As(V) (Fig. 6E).

V. paradoxus strain IDSBO-4 exhibited both Sb(III) oxidation and As(III) oxidation in the air but did not oxidize either electron donor with nitrate as a terminal electron acceptor under anoxic conditions. Figure 7A shows that IDSBO-4 removed 0.4 mM $C_8H_4K_2O_{12}Sb_2{\cdot}3H_2O$ from solution in aerobic cultures after 10 days with 61% recovery of the associated 1 mM Sb(III) as aqueous Sb(V) and a corresponding 7-fold increase in cell density. Likewise, 0.6 mM $KNaC_4H_4O_6{\cdot}4H_2O$ supported a similar 9-fold increase in cell growth of IDSBO-4 with 86% utilization of the substrate within 10 days (Fig. 7B). As with strain IDSBO-1, live Sb(III)-amended tubes developed a white mineral precipitate, which was identified by XRD as senarmontite (data not shown). Arsenic(III) (0.81 mM) was oxidized to As(V) in 10 days by IDSBO-4 in the air, with a corresponding 6-fold increase in cell density (Fig. 7C). When $C_8H_4K_2O_{12}Sb_2{\cdot}3H_2O$ and As(III) were both provided, aerobic cultures of strain IDSBO-4 oxidized Sb(III) and As(III) concomitantly. Figure 7D shows that within 10 days, these cultures oxidized 0.6 mM $C_8H_4K_2O_{12}Sb_2{\cdot}3H_2O$ [corresponding to an Sb(III) concentration of 1.2 mM] with an aqueous recovery of 0.8 mM Sb(V). Hence, the rate of $C_8H_4K_2O_{12}Sb_2{\cdot}3H_2O$ utilization in the coamended culture (Fig. 7D) was very similar to that in the culture that received only $C_8H_4K_2O_{12}Sb_2{\cdot}3H_2O$ (Fig. 7A). The rate of Sb(V) production during growth on $C_8H_4K_2O_{12}Sb_2{\cdot}3H_2O$, however, was nearly twice as high in the coamended culture as that with $C_8H_4K_2O_{12}Sb_2{\cdot}3H_2O$ only. The rate of As(III) oxidation to As(V) in the coamended culture was also nearly twice that of the culture that received As(III) only (Fig. 7C). Cell growth in the coamended culture demonstrated a 9-fold increase in cell density over 10 days, a rate comparable to those of the other IDSBO-4 cultures that contained tartrate compounds without As(III) (Fig. 7A and B). No loss of tartrate compounds or oxidation of Sb(III) or As(III) occurred in tubes that were autoclaved after inoculation, and no growth of IDSBO-4 was observed in control tubes that lacked Sb(III) or As(III) amendment (data not shown).

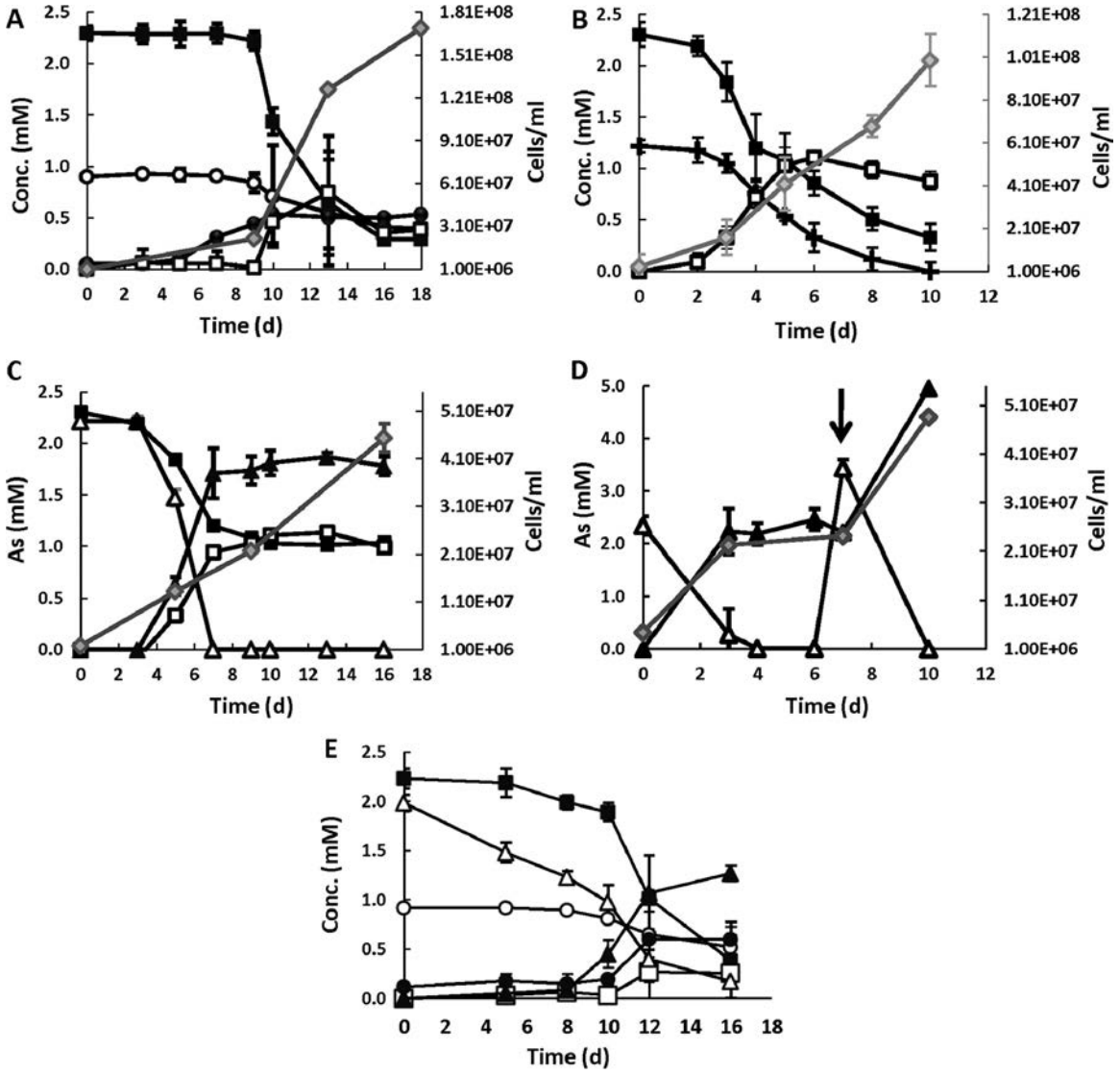

FIG 6 Oxidation of Sb(III) and As(III) during growth of *H. taeniospiralis* strain IDSBO-1. (A to E) $C_8H_4K_2O_{12}Sb_2{\cdot}3H_2O$ as the electron donor and nitrate as the electron acceptor under anaerobic conditions (A), $KNaC_4H_4O_6{\cdot}4H_2O$ as the electron donor and nitrate as the electron acceptor under anaerobic conditions (B), autotrophic growth with As(III) as the electron donor and nitrate as the electron acceptor under anaerobic conditions (C), autotrophic growth with As(III) as the electron donor under aerobic conditions (D), and sequential oxidation of As(III) and Sb(III) with nitrate in coamended cultures of strain IDSBO-1 (E). Open circles represent $C_8H_4K_2O_{12}Sb_2{\cdot}3H_2O$, closed circles represent Sb(V), crosses represent $KNaC_4H_4O_6{\cdot}4H_2O$, open triangles represent As(III), closed triangles represent As(V), closed squares represent nitrate, open squares represent nitrite, and gray diamonds represent cells. An arrow denotes the timing of supplemental As(III) amendment. Symbols represent the means from three replicate samples, and error bars represent ±1 standard deviation. The absence of bars indicates that the error was smaller than the sample.

Radioisotope experiments. *V. paradoxus* strain IDSBO-4 demonstrated the fixation of [^{14}C]bicarbonate into cell material that was coupled to the oxidation of Sb(III) or As(III). Cells that were incubated in the dark for 6 days under aerobic conditions in the presence of 2 mM Sb(III) incorporated 0.15% ± 0.002% (n = 3) of the added $H^{14}CO_3^-$ radiotracer compared to 0.01% ± 0.001% incorporation in Sb(III)-free tubes (n = 3). Radiotracer incorporation was also stimulated in tubes amended with 2 mM As(III), which incorporated 0.06% ± 0.007% of the added $H^{14}CO_3^-$ (n = 3). A thin layer of white mineral precipitate formed in all Sb(III)-amended tubes, including abiotic control tubes, which lacked cells, but the residue did not incorporate measurable ^{14}C (radiotracer recovery was 0.01% ± 0.002%). We did not test strain IDSBO-1 for the ability to fix [^{14}C]bicarbonate.

DISCUSSION

This study demonstrates a novel pathway for microbiological Sb(III) oxidation that has been previously described for As(III) oxidation, namely, the anaerobic oxidation of Sb(III) coupled to the reduction of nitrate by our isolate *H. taeniospiralis* strain IDSBO-1 (Fig. 6A). Furthermore, our experiments demonstrating cellular incorporation of [^{14}C]bicarbonate during aerobic Sb(III) oxidation by *V. paradoxus* strain IDSBO-4 suggest the possibility of Sb(III)-based chemoautotrophy in that organism, a metabolic

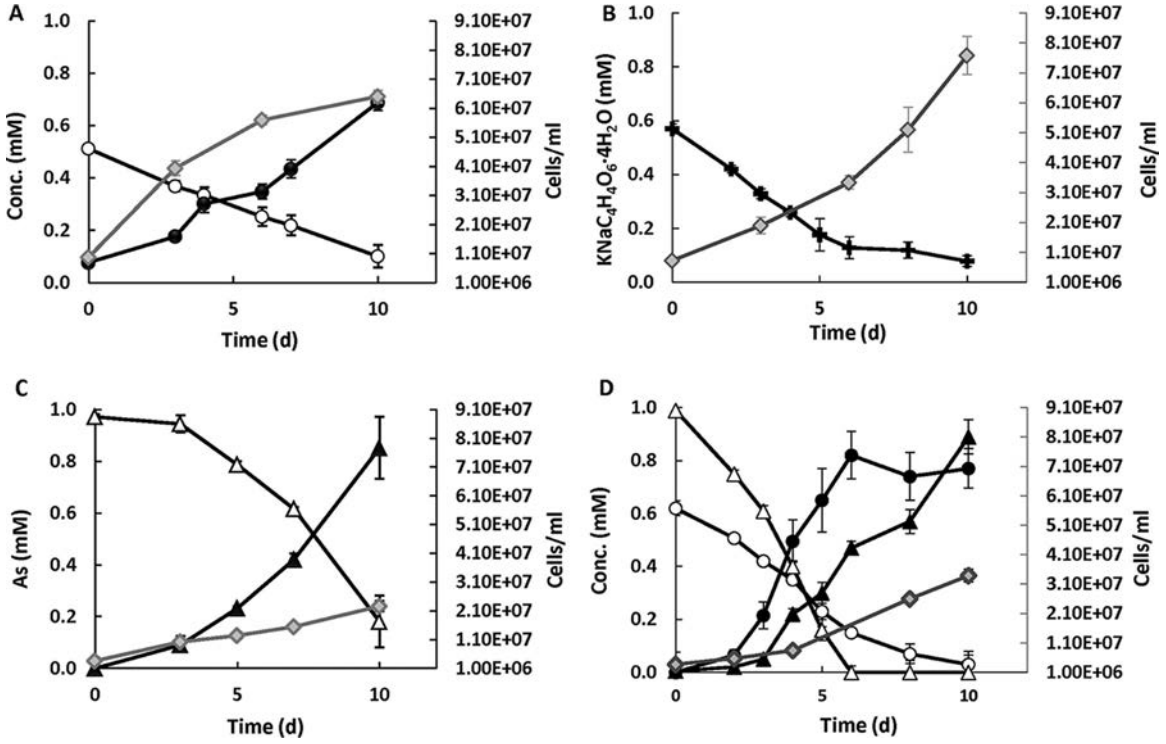

FIG 7 Oxidation of Sb(III) and As(III) and growth of *V. paradoxus* strain IDSBO-4 under aerobic conditions with $C_8H_4K_2O_{12}Sb_2{\cdot}3H_2O$ as the electron donor (A), $KNaC_4H_4O_6{\cdot}4H_2O$ as the electron donor (B), As(III) as the electron donor (C), and coamendment with $C_8H_4K_2O_{12}Sb_2{\cdot}3H_2O$ and As(III) (D). Open circles represent $C_8H_4K_2O_{12}Sb_2{\cdot}3H_2O$, closed circles represent Sb(V), crosses represent $KNaC_4H_4O_6{\cdot}4H_2O$, open triangles represent As(III), closed triangles represent As(V), and gray diamonds represent cells. Symbols represent the means from three replicate samples, and error bars represent ±1 standard deviation. The absence of bars indicates that the error was smaller than the sample.

process that is of known environmental significance with respect to As cycling (9, 10). On the other hand, our experiments demonstrating growth of both of these isolates on sodium tartrate ($KNaC_4H_4O_6{\cdot}4H_2O$) in the absence of Sb or As (Fig. 6B and 7B) illustrate a significant "pitfall" of using the commonly utilized Sb(III)-tartrate ($C_8H_4K_2O_{12}Sb_2{\cdot}3H_2O$) as a source for soluble Sb(III) in studies of autotrophy.

In recent years, our emerging picture of the geomicrobiological Sb cycle has revealed distinct similarities to that of As. Bacterial processes are known to mediate oxidative and reductive transformations of both metalloids between their environmentally relevant trivalent and pentavalent oxidation states. In As-rich environments microbiological processes represent the primary environmental pathway for As(III) oxidation to As(V), a reaction that otherwise occurs slowly under oxic conditions (48). *In situ* rates of microbiological Sb oxidation in contaminated settings have yet to be measured, but recent work in the laboratory with Sb-resistant heterotrophic microbial consortia (25) and bacterial isolates (26–28) suggest that this behavior is phylogenetically widespread. It has been elicited in bacteria isolated from Sb-impacted mine soils (25, 27) and industrially contaminated aquatic sediments (28).

In these recent studies, the Sb(III)-oxidizing bacteria that have been described are heterotrophs and were not shown to conserve energy for growth from the reaction (25–28). Instead, the Sb(III) oxidation activity appears to have been associated with cellular Sb(III) resistance mechanisms (26, 27) similar to those employed by some As-resistant heterotrophic prokaryotes that oxidize As(III) (9). The first identified Sb(III)-oxidizing bacterium, *Stibiobacter senarmontii*, was isolated from an Sb ore deposit in Yugoslavia during the late 1970s and is described in the English-language literature in an article by Lyalikova (31). In that study, *S. senarmontii* was reported to grow as an autotroph under oxic conditions using Sb(III) as an electron donor, as demonstrated by [^{14}C]bicarbonate fixation experiments. The source of Sb(III) used in those experiments was solid antimony trioxide (Sb_2O_3). The oxidation of Sb(III) by *S. senarmontii* resulted in the precipitation of the Sb(V)- and Sb(III)-bearing oxide mineral stibiconite [$Sb_3O_6(OH)$]. However, growth rates for *S. senarmontii* were not quantified, and the enzymatic pathways of Sb(III)-based autotrophy in that organism were not explored. To our knowledge, the *S. senarmontii* cell line has since been lost.

The results of our sediment microcosm experiments (Fig. 1) demonstrate oxidation of As(III) to As(V), as well as the biological removal of Sb(III) from solution, by the sedimentary microbial community around Stibnite Mine. The lack of activity in autoclaved controls indicates that these processes are biologically mediated. In general agreement with Lyalikova's results (31), our experiments with enrichment cultures of Sb(III)-oxidizing bacteria from these sediments demonstrated the precipitation and sequestration of Sb during oxidation as an insoluble Sb(V)-oxide mineral (mopungite), along with lesser amounts of Sb(III)-bearing senarmontite (Fig. 2 and 3). The equilibrium phases of Sb at circumneutral pH are much less soluble than analogous As phases (49), and a growing body of literature suggests that bioprecipita-

tion of Sb-bearing mineral phases also occurs during microbiological Sb(V) reduction (23, 24).

In the decades following Lyalikova's work, microbiological Sb(III) oxidation went largely unexplored until Lehr and others (26) investigated the process in an As(III)-oxidizing strain of *Agrobacterium tumefaciens*. They found that the wild type of *A. tumefaciens* as well as two *aio* mutant strains that were incapable of As(III) oxidation could all oxidize Sb(III) and concluded that Sb(III) oxidation and As(III) oxidation are catalyzed by distinct enzymatic pathways. Subsequent work involving some of the same investigators (32), however, found that under varied culturing conditions a partial inhibition of Sb(III) oxidation was observed in the *aio* mutants. This suggests that *aio* gene products may indeed be partially involved in Sb(III) oxidation (32). In this study, phylogenetic analysis of *aioA* sequences amplified and sequenced from strains IDSBO-1 and IDSBO-4 revealed that the two bacteria possess very similar AioA aerobic oxidase proteins on a node with 90% bootstrap support and cluster with AioA from other As(III)-oxidizing *Betaproteobacteria* (Fig. 5). The AioA from Strain IDSBO-1 was also closely related to that of *Acidovorax* sp. strain NO1, residing on a node with 87% bootstrap support. *Acidovorax* sp. strain NO1 is unique among all sequenced strains of *Acidovorax* in being the only known representative of that genus to possess the *aio* operon for As(III) oxidation, along with two adjacent *ars* resistance operons (50). It is not known whether *Acidovorax* sp. strain NO1 shares the capacity of *H. taeniospiralis* strain IDSBO-1 to oxidize Sb(III).

The *aioAB* operon for aerobic As(III) oxidation was previously found to be expressed by As(III) but not by Sb(III) in *A. tumefaciens* (32). This is supported by our finding that strain IDSBO-1 demonstrated growth coupled to the oxidation of As(III) in the air (Fig. 6D) or under anoxic conditions with nitrate (Fig. 6C) but oxidized Sb(III) only under anoxic conditions (Fig. 6A). We did not screen for other As structural genes in this study, and further work is necessary to determine if the *arx* operon that encodes anaerobic As(III) oxidation is also involved in anaerobic Sb(III) oxidation. Strain IDSBO-4, in contrast, grew while oxidizing As(III) (Fig. 7A) and Sb(III) (Fig. 7C) only as an aerobe. The observed Sb(III) oxidation in the absence of As(III) suggests the involvement of other, novel biochemical pathways that are expressed in the presence of Sb(III). A comparison of all potential CISMs encoded in the genomes of strains IDSBO-1 and IDSBO-4 to those of closely related organisms that cannot oxidize Sb(III) could facilitate the discovery of novel, specific enzymes for Sb(III) oxidase. We note that a recent study by Li et al. (33) has identified such a novel operon, denoted *anoA*, that encodes an Sb(III) oxidase that is expressed in *A. tumefaciens* by the presence of Sb(III). The authors of that study note that other unknown enzymes appear to be involved in Sb(III) oxidation in *A. tumefaciens* as well.

The preferential anaerobic oxidation of As(III) prior to Sb(III) by strain IDSBO-1 when both electron donors were provided concomitantly (Fig. 6E) may indicate that the former anion acted as a preferred electron donor for chemoautotrophy. Alternately, it may suggest that the genetic pathways involved in As(III)- and Sb(III)-dependent denitrification oxidize As(III) more efficiently than Sb(III). The initiation of Sb(III) oxidation prior to the complete oxidation and depletion of As(III) in this experiment suggests that the relative environmental concentrations of the two anions influence the expression of Sb(III) oxidation. The preferential utilization of As(III) by these bacteria cannot be explained by enzymatic preconditioning in our isolated strains, as the cell lines used in the coamended experiments were grown on Sb(III) and were not exposed to As(III) during previous culturing. The preference for As(III) over Sb(III) by these organisms may reflect a generally higher concentration of As compared to Sb in the Stibnite Mine ecosystem. Nevertheless, the rapid onset of As(III) oxidation without a significant lag time by the Sb(III)-adapted strains demonstrates a capacity to rapidly change from Sb(III) to As(III) oxidation. This could indicate that some common enzymes (e.g., Arx and Aio) are involved in the oxidation of both metalloids and may be constitutive during Sb(III)-based chemoautotrophy; however, further work will be required to address this question.

Strain IDSBO-4 oxidized As(III) and Sb(III) simultaneously when both electron donors were provided (Fig. 7D). The rate of cell growth in the coamended culture was similar to that measured when strain IDSBO-4 was amended with only $C_8H_4K_2O_{12}Sb_2{\cdot}3H_2O$ (Fig. 7A) or with $KNaC_4H_4O_6 \cdot 4H_2O$ (Fig. 7B). This suggests that heterotrophic growth on tartrate, rather than As(III)- or Sb(III)-dependent autotrophy, was likely the predominant metabolic process in these coamended cultures. However, the cell yield after 10 days was markedly higher when cells were grown with $C_8H_4K_2O_{12}Sb_2{\cdot}3H_2O$ (Fig. 7A) or with $KNaC_4H_4O_6{\cdot}4H_2O$ (Fig. 7B) than with As(III) (Fig. 7C) or As(III) plus $C_8H_4K_2O_{12}Sb_2{\cdot}3H_2O$ (Fig. 7D). The cause of this inhibition in the presence of As is not clear, but it may be related to a buildup of As(V) or to the combination of the two toxic trivalent anions themselves. It is notable that Sb(III) oxidation occurred much more rapidly in the coamended culture (Fig. 7D) than in the culture that received Sb(III) only (Fig. 7A). This may represent the expression and involvement of *aio* or other unidentified operons for Sb(III) oxidation by the presence of As(III), as suggested previously by Wang et al. (32).

In conclusion, the contamination of freshwater ecosystems with Sb is likely to continue to grow in importance as an environmental concern because the metalloid is increasingly being used in a diverse array of products and industries. A more detailed understanding of the geomicrobiological Sb cycle is necessary to predict and manage the behavior of Sb in impacted settings. The results of this study confirm recent reports that biological Sb(III) oxidation can be readily elicited from bacterial populations in Sb- and As-contaminated settings (25–28). This process can exert a strong influence over the precipitation and sequestration of Sb in the form of insoluble mineral phases under both oxic and anoxic conditions. Future studies should focus on growing these and other Sb(III)-oxidizing organisms with a tartrate-free Sb(III) source, such as solid antimony trioxide, to confirm whether the observed growth is indeed linked to Sb(III)-dependent autotrophy. Further genetic sequencing and proteomic studies of these isolates would also be highly useful to identify potential new structural genes that encode bacterial Sb(III) oxidation.

ACKNOWLEDGMENTS

We thank David Pilliod and Robert Arkle (USGS-BRD) for invaluable assistance with field work and sampling. We are very grateful to Matthew Parker (Binghamton University) for assistance with molecular biological methods and to David Jenkins (Binghamton University) for assistance with XRD.

REFERENCES

1. **Filella M, Belzile N, Chen Y.** 2002. Antimony in the environment: a review focused on natural waters. I. Occurrence. Earth-Sci Rev **57:**125–176. http://dx.doi.org/10.1016/S0012-8252(01)00070-8.
2. **Fu Z, Wu F, Mo C, Liu B, Zhu J, Deng Q, Liao H, Zhang Y.** 2010. Bioaccumulation of antimony, arsenic, and mercury in the vicinities of a large antimony mine, China. Microchem J **97:**12–19.
3. **Krachler M, Emons H, Zheng J.** 2001. Speciation of antimony for the 21st century: promises and pitfalls. Trends Anal Chem **20:**79–90. http://dx.doi.org/10.1016/S0165-9936(00)00065-0.
4. **Murciego AM, Sánchez AG, González MAR, Gil EP, Gordillo CT, Fernández JC, Triguero TB.** 2007. Antimony distribution and mobility in topsoils and plants (*Cytisus striatus*, *Cistus ladanifer* and *Dittrichia viscosa*) from polluted Sb-mining areas in Extremadura (Spain). Environ Pollut **145:**15–21. http://dx.doi.org/10.1016/j.envpol.2006.04.004.
5. **Culioli J, Fouquoire A, Mori C, Orsini A.** 2009. Trophic transfer of arsenic and antimony in a freshwater ecosystem: a field study. Aquat Toxicol **94:**286–293. http://dx.doi.org/10.1016/j.aquatox.2009.07.016.
6. **Dovick MA, Kulp TR, Arkle R, Pilliod D.** 13 October 2015. Bioaccumulation trends of arsenic and antimony in a freshwater ecosystem affected by mine drainage. Environ Chem http://dx.doi.org/10.1071/EN15046.
7. **Liu F, Le XC, McKnight-Whitford A, Xia Y, Wu F, Elswick E, Johnson CC, Zhu C.** 2010. Antimony speciation and contamination of waters in the Xikuangshan antimony mining and smelting area, China. Environ Geochem Health **32:**401–413. http://dx.doi.org/10.1007/s10653-010-9284-z.
8. **Telford K, Maher W, Krikowa F, Foster S, Ellwood MJ, Ashley PM, Lockwood PV, Wilson SC.** 2009. Bioaccumulation of antimony and arsenic in a highly contaminated stream adjacent to the Hillgrove Mine, NSW, Australia. Environ Chem **6:**133–143. http://dx.doi.org/10.1071/EN08097.
9. **Oremland RS, Stolz J.** 2003. The ecology of arsenic. Science **300:**939–944. http://dx.doi.org/10.1126/science.1081903.
10. **Zhu YG, Yoshinaga M, Zhao FJ, Rosen BP.** 2014. Earth abides arsenic biotransformations. Annu Rev Earth Planet Sci Lett **42:**443–467. http://dx.doi.org/10.1146/annurev-earth-060313-054942.
11. **Cai J, Salmon K, DuBow MS.** 1998. A chromosomal ars operon homologue of *Pseudomonas aeruginosa* confers increased resistance to arsenic and antimony in *Escherichia coli*. Microbiology **144:**2705–2729. http://dx.doi.org/10.1099/00221287-144-10-2705.
12. **Meng YL, Liu Z, Rosen BP.** 2004. As(III) and Sb(III) uptake by GlpF and efflux by ArsB in Escherichia coli. J Biol Chem **279:**18334–18341. http://dx.doi.org/10.1074/jbc.M400037200.
13. **Mukhopadhyay R, Rosen BP, Phung LT, Silver S.** 2002. Microbial arsenic: from geocycles to genes and enzymes. FEMS Microbiol Rev **26:**311–325. http://dx.doi.org/10.1111/j.1574-6976.2002.tb00617.x.
14. **Oremland RS, Hoeft SE, Santini JM, Bano N, Hollibaugh RA, Hollibaugh JT.** 2002. Anaerobic oxidation of arsenite in Mono Lake water and by a facultative, arsenite-oxidizing chemoautotroph, strain MLHE-1. Appl Environ Microbiol **68:**4795–4802. http://dx.doi.org/10.1128/AEM.68.10.4795-4802.2002.
15. **Richey C, Chovanec P, Hoeft SE, Oremland RS, Basu P, Stolz JF.** 2009. Respiratory arsenate reductase as a bidirectional enzyme. Biochem Biophys Res Commun **382:**298–302. http://dx.doi.org/10.1016/j.bbrc.2009.03.045.
16. **Budinoff CR, Hollibaugh JT.** 2008. Arsenite-dependent photoautotrophy by an *Ectothiorhodospira*-dominated consortium. ISME J **2:**340–343. http://dx.doi.org/10.1038/ismej.2007.115.
17. **Kulp TR, Hoeft SE, Asao M, Madigan MT, Hollibaugh JT, Fisher JC, Stolz JF, Culbertson CW, Miller LG, Oremland RS.** 2008. Arsenic(III) fuels anoxygenic photosynthesis in hot spring biofilms from Mono Lake, California. Science **321:**967–970. http://dx.doi.org/10.1126/science.1160799.
18. **Hoeft SE, Kulp TR, Han S, Lanoil B, Oremland RS.** 2010. Coupled arsenotrophy in a hot spring photosynthetic biofilm at Mono Lake, California. Appl Environ Microbiol **76:**4633–4639. http://dx.doi.org/10.1128/AEM.00545-10.
19. **Zargar K, Hoeft SE, Oremland RS, Saltikov CW.** 2010. Identification of a novel arsenite oxidase gene, arxA, in the haloalkaliphilic, arsenite-oxidizing bacterium *Alkalilimnicola ehrlichii* strain MLHE-1. J Bacteriol **192:**3755–3762. http://dx.doi.org/10.1128/JB.00244-10.
20. **Zargar K, Conrad A, Bernick DL, Lowe TM, Stolc V, Hoeft S, Oremland RS, Stolz J, Saltikov CW.** 2012. ArxA, a new clade of arsenite oxidase within the DMSO reductase family of molybdenum oxidoreductases. Environ Microbiol **14:**1635–1645. http://dx.doi.org/10.1111/j.1462-2920.2012.02722.x.
21. **Hille R, Hall J, Basu P.** 2014. The mononuclear molybdenum enzymes. Chem Rev **114:**3963–4038. http://dx.doi.org/10.1021/cr400443z.
22. **Rothery RA, Workun GJ, Weiner JH.** 2008. The prokaryotic complex iron-sulfur molybdoenzyme family. Biochim Biophys Acta **1778:**1897–1929. http://dx.doi.org/10.1016/j.bbamem.2007.09.002.
23. **Abin CA, Hollibaugh JT.** 2014. Dissimilatory antimonate reduction and production of antimony trioxide microcrystals by a novel microorganism. Environ Sci Technol **48:**681–688. http://dx.doi.org/10.1021/es404098z.
24. **Kulp TR, Miller LG, Braiotta F, Webb SM, Kocar BD, Blum JS, Oremland RS.** 2014. Microbiological reduction of Sb(V) in anoxic freshwater sediments. Environ Sci Technol **48:**218–226. http://dx.doi.org/10.1021/es403312j.
25. **Hamamura N, Fukushima K, Itai T.** 2013. Identification of antimony- and arsenic-oxidizing bacteria associated with antimony mine tailing. Microbes Environ **28:**257–263. http://dx.doi.org/10.1264/jsme2.ME12217.
26. **Lehr CR, Kashyap DR, McDermott TR.** 2007. New insights into microbial oxidation of antimony and arsenic. Appl Environ Microbiol **73:**2386–2389. http://dx.doi.org/10.1128/AEM.02789-06.
27. **Li J, Wang Q, Zhang S, Qin D, Wang G.** 2013. Phylogenetic and genome analyses of antimony-oxidizing bacteria isolated from antimony mined soil. Int Biodeter Biodegr **76:**76–80. http://dx.doi.org/10.1016/j.ibiod.2012.06.009.
28. **Nguyen VK, Lee JU.** 2015. Antimony-oxidizing bacteria isolated from antimony contaminated sediment—a phylogenetic study. Geomicrobiol J **32:**50–58. http://dx.doi.org/10.1080/01490451.2014.925009.
29. **Lialikova NN.** 1974. *Stibiobacter senarmontii*—a new microorganism oxidizing antimony. Mikrobiologiia **43:**941–948. (In Russian; English translation, p 799–805.)
30. **Lyalikova NN, Vedenina IY, Romanova AK.** 1976. Assimilation of carbon-dioxide by a culture of *Stibiobacter senarmontii*. Mikrobiologiia **45:**476–477. (In Russian; English translation, p 476–477.)
31. **Lyalikova NN.** 1978. Antimony-oxidizing bacteria and their geochemical activity. Environ Biogeochem Geomicrobiol **3:**929–936.
32. **Wang Q, Warelow TP, Kang YS, Romano C, Osborne TH, Lehr CR, Bothner B, McDermott TR, Santini JM, Wang G.** 2015. Arsenite oxidase also functions as an antimonite oxidase. Appl Environ Microbiol **81:**1959–1965. http://dx.doi.org/10.1128/AEM.02981-14.
33. **Li J, Wang Q, Li M, Yang B, Shi M, Guo W, McDermott T, Rensing C, Wang G.** 2015. Proteomics and genetics for identification of a bacterial antimonite oxidase in *Agrobacterium tumefaciens*. Environ Sci Technol **49:**5980–5989. http://dx.doi.org/10.1021/es506318b.
34. **Jin L.** 2003. Public health assessment Stibnite/Yellow Pine mining area. Public health assessments & health consultations. Agency for Toxic Substances and Disease Registry, Atlanta, GA. http://www.atsdr.cdc.gov/HAC/pha/pha.asp?docid=1060&pg=1.
35. **Oremland RS, Blum JS, Culbertson CW, Visscher PT, Miller LG, Dowdle P, Strohmaier FE.** 1994. Isolation, growth, and metabolism of an obligately anaerobic, selenate-respiring bacterium, strain SES-3. Appl Environ Microbiol **60:**3011–3019.
36. **Wolin EA, Wolin M, Wolfe RS.** 1963. Formation of methane by bacterial extracts. J Biol Chem **238:**2882–2886.
37. **Miller LG, Baesman SM, Kirshtein J, Voytek MA, Oremland RS.** 2013. A biogeochemical and genetic survey of acetylene fermentation by environmental samples and bacterial isolates. Geomicrobiol J **30:**501–516. http://dx.doi.org/10.1080/01490451.2012.732662.
38. **Hungate RE.** 1969. Chapter IV. A roll tube method for cultivation of strict anaerobes. Methods Microbiol **3:**117–132.
39. **Hobbie JE, Daley RJ, Jasper S.** 1977. Use of nuclepore filters for counting bacteria by fluorescence microscopy. Appl Environ Microbiol **33:**1225–1228.
40. **Hoeft SE, Lucas FO, Hollibaugh JT, Oremland RS.** 2002. Characterization of microbial arsenate reduction in the anoxic bottom waters of Mono Lake, California. Geomicrobiol J **19:**23–40. http://dx.doi.org/10.1080/014904502317246147.
41. **Polz MF, Cavanaugh CM.** 1998. Bias in template-to-product ratios in multitemplate PCR. Appl Environ Microbiol **64:**3724–3730.
42. **Inskeep WP, Macur RE, Hamamura N, Warelow TP, Ward SA, Santini JM.** 2007. Detection, diversity and expression of aerobic bacterial arsenite oxidase genes. Environ Microbiol **9:**934–943. http://dx.doi.org/10.1111/j.1462-2920.2006.01215.x.
43. **Tamura K, Peterson D, Peterson N, Stecher G, Nei M, Kumar S.** 2011.

MEGA5: molecular evolutionary genetics analysis using maximum likelihood, evolutionary distance, and maximum parsimony methods. Mol Biol Evol **28:**2731–2739. http://dx.doi.org/10.1093/molbev/msr121.
44. **Felsenstein J.** 1985. Confidence limits on phylogenies: an approach using the bootstrap. Evolution **39:**783–791. http://dx.doi.org/10.2307/2408678.
45. **Edgar RC.** 2004. MUSCLE: multiple sequence alignment with high accuracy and high throughput. Nucleic Acids Res **32:**1792–1797. http://dx.doi.org/10.1093/nar/gkh340.
46. **Whelan S, Goldman N.** 2001. A general empirical model of protein evolution derived from multiple protein families using a maximum-likelihood approach. Mol Biol Evol **18:**691–699. http://dx.doi.org/10.1093/oxfordjournals.molbev.a003851.
47. **Wang Q, Garrity GM, Tiedje JM, Cole JR.** 2007. Naïve Bayesian classifier for rapid assignment of rRNA sequences into the new bacterial taxonomy. Appl Environ Microbiol **73:**5261–5267. http://dx.doi.org/10.1128/AEM.00062-07.
48. **Leuz AK, Johnson CA.** 2005. Oxidation of Sb(III) to Sb(V) by O_2 and H_2O_2 in aqueous solutions. Geochim Cosmochim Acta **69:**1165–1172. http://dx.doi.org/10.1016/j.gca.2004.08.019.
49. **Vink BW.** 1996. Stability relations of antimony and arsenic compounds in the light of revised and extended Eh-pH diagrams. Chem Geol **130:**21–30. http://dx.doi.org/10.1016/0009-2541(95)00183-2.
50. **Huang Y, Li H, Rensing C, Zhao K, Johnstone L, Wang G.** 2012. Genome sequence of the facultative anaerobic arsenite-oxidizing and nitrate-reducing bacterium *Acidovorax* sp. strain NO1. J Bacteriol **194:**1635–1636. http://dx.doi.org/10.1128/JB.06814-11.
51. **Hoeft SE, Kulp TR, Stolz JF, Hollibaugh JT, Oremland RS.** 2004. Dissimilatory arsenate reduction with sulfide as electron donor: experiments with Mono Lake water and isolation of strain MLMS-1, a chemoautotrophic arsenate respirer. Appl Environ Microbiol **70:**2741–2747. http://dx.doi.org/10.1128/AEM.70.5.2741-2747.2004.